JOURNAL OF MATERIALS SCIENCE 14 (1979) 1662–1668

The crack-initiation threshold in ceramic materials subject to elastic/plastic indentation

JAMES LANKFORD, DAVID L. DAVIDSON
Southwest Research Institute, San Antonio, Texas, USA

The threshold for indentation cracking is established for a range of ceramic materials, using the techniques of scanning electron microscopy and acoustic emission. It is found that by taking into account indentation plasticity, current theories may be successfully combined to predict threshold indentation loads and crack sizes. Threshold cracking is seen to relate to radial rather than median cracking.

1. Introduction

The impact of small, hard particles upon the surfaces of engineering ceramics often causes indentation cracking, which can degrade the mechanical properties of the target in two major areas: (1) erosion resistance, and (2) tensile strength. In order to optimize operating performance, it is important to know the parameters, i.e. load, crack size, crack shape, corresponding to the threshold for damage in a given ceramic, as well as the influence of deformation and fracture properties in establishing this threshold for a given ceramic. Currently, there appears to exist no reliable experimental data concerning indentation threshold damage parameters in ceramics. However, recent progress has been made in the theoretical consideration of the influence of both the elastic/plastic indentation stress field, and material deformation/fracture properties, upon the threshold for indentation cracking.

In particular, Lawn and Evans [1] have developed a model to determine the critical conditions for the initiation of cracks at the sites of sharp indenters. The model uses a very simplified approximation to the elastic/plastic stress field of an actual indentation, i.e. one based upon the solution for an expanding cavity, and as a consequence predicts that the initial cracks formed will be "median" (subsurface, penny-shaped) flaws lying at the elastic/plastic boundary beneath the apex of the indenter. From a fracture-mechanics-based analysis utilizing this stress field representation, the sizes of the earliest formed cracks, and their corresponding indenter loads, are predicted for a range of ceramic materials.

Another recent model, developed principally to describe Palmqvist* cracking in tough ceramics like WC–Co, has been proposed by Perrott [2]. In this case, account is taken of the fact that the stress distribution on the indenter/indentation interface is not really constant, but rather is a function of the indentation plastic zone size. Because of this stress redistribution, the maximum tensile field occurs near the surface, at the indent corners, rather than below the indentation apex as in the Lawn–Evans model. Thus the Perrott theory predicts radial, rather than median, crack nucleation. Unlike the Lawn–Evans theory, the Perrott model does not rank materials in terms of their critical crack nucleation parameters, threshold load and crack size.

In this paper, the results of an experimental study of threshold crack nucleation in a wide range of ceramics are described. It is shown that by considering the two existing theoretical models in combination, the materials studied may be ranked successfully in terms of their relative threshold crack sizes and loads; further, both parameters may be predicted with surprising accuracy.

2. Experimental procedure

The materials chosen consisted of single-crystal

*Palmqvist cracks are shallow, radial surface fractures lying within median planes (i.e. planes containing the axis of the indenter), extending out from the corners of an indentation.

0022–2461/79/071662–07 $2.70/0

TABLE I

Material	Deformation/fracture parameters		Threshold parameters				
	H(GPa)	K_c(MPa m$^{1/2}$)	P^*_{theory}(g)	P^*_{theory}(g) (corrected)	P^*_{exp}(g)	c^*_{theory}(μm)	c^*_{exp}(μm)
NaCl (crystal)	0.24	0.5	4000	725	1500	120	100
Al_2O_3 (poly)	12	4	300	26	25	5	3
SiC (poly)	19	4	80	8	10	2.0	1.0
Si (crystal)	10	0.6	0.3	2.5†	5(3‡)	0.2	0.65
Ge (crystal)	9	0.46	0.15	1.25†	2.0	0.14	0.25

† $\eta = 0.1$ rather than 1.0.
‡ Experimental result of Sata *et al.* [7].

sodium chloride, silicon, and germanium, and polycrystalline aluminium oxide† and silicon carbide‡. These provided a wide range in electronic bonding type and deformation/fracture properties, as indicated in Table I. Faces of the NaCl crystal were {1 0 0} as-cleaved surfaces, while the silicon and germanium crystals had as-grown surfaces. The Al_2O_3 and SiC specimen surfaces were polished to a 0.25 μm diamond finish.

Acoustic emission (AE) was monitored using an apparatus (described previously [3]) operating within the frequency domain 100 kHz to 1 MHz, using a PZT transducer resonant at 160 kHz. During the microhardness tests, the specimens rested on an alumina base, to which the transducer was affixed.

Microhardness tests were carried out over a load range of 1 to 6000 g; during each test, the quasi-statically applied, diamond pyramid indenter rested upon the specimen for approximately 18 secs. The threshold for indentation cracking was determined to correspond to the lowest load at which acoustic emission could be detected. At all loads at which emission occurred, optical or electron microscopy was used to verify the presence of, and measure, indentation cracks. Similarly, the SEM was used to ensure that "quite" (no AE) indentations were crack-free. For observation in the SEM, it was necessary to coat the Al_2O_3 specimens with a thin, conducting film of palladium.

3. Results

Deformation/fracture phenomena characteristic of the indentation threshold are shown in Figs. 1 and 2. In Fig. 1, both NaCl indents were produced by 1500 g loads. Since this is the approximate threshold load for this material, the presence of

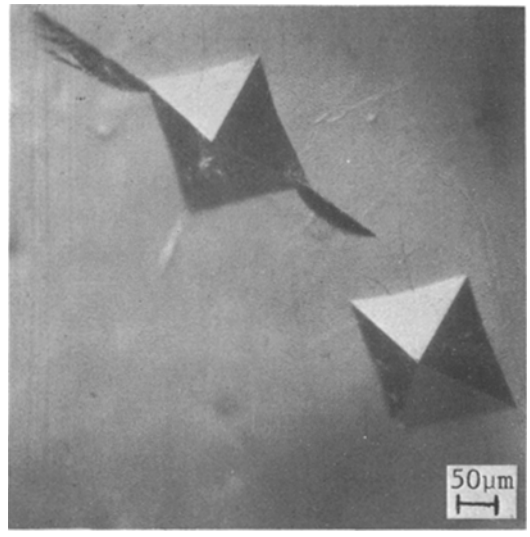

Figure 1 Indents on as-cleaved {1 0 0} face of NaCl crystal, indent diagonals parallel to ⟨1 1 0⟩, both indents caused by 1500 g load, with radial cracks nucleated adjacent to the upper indent, optical view at × 55.

cracks is very sensitive to the local microflaw population in the vicinity of each indent corner. Thus, only one of the indents displays cracks, and these at only three of the corners; clearly, the only cracks are radial, with no subsurface median cracks visible in this transparent material. In this particular case, acoustic emission was associated only with the cracked indentation. It is interesting to observe that the NaCl formed indentation cracks only when oriented such that the indentation diagonals were approximately parallel to ⟨1 1 0⟩; when rotated 45°, so that the diagonals were parallel to ⟨1 0 0⟩, no cracks were obtained for loads as high as 6000 g, the maximum capacity of the microhardness tester. Similar crystallographic

†Lucalox, 25 μm grain size, General Electric Lamp Glass Division, Cleveland, Ohio, USA.
‡Sintered α-SiC, 7 μm grain size, Carborundum Corporation, Niagara Falls, New York, USA.

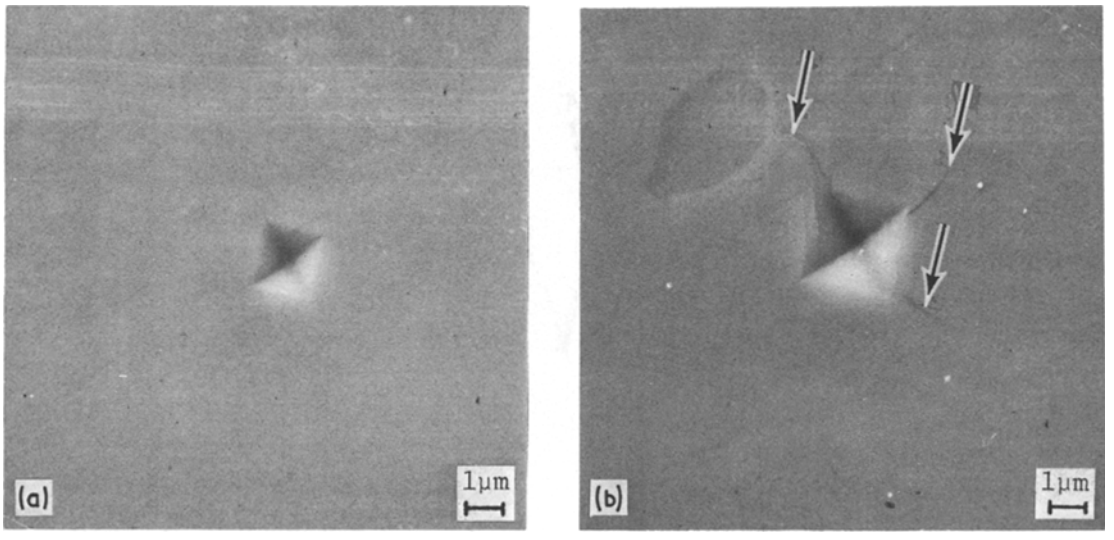

Figure 2 Indents on polished surface of polycrystalline Al_2O_3, SEM view at × 2800. (a) 25 g load, no cracking. (b) 50 g load, radial cracking (arrow), twins formed.

dependencies of indentation cracking have been noted [4] for other ionic solids as well.

The near threshold behaviour of aluminium oxide is shown in Fig. 2. In Fig. 2a, a 25 g load is seen to produce a perfect indentation, with no visible cracks. Acoustic emission did not occur during the formation of this indent. Cracking and acoustic emission both were detected, however, at the site of the 50 g indentation shown in Fig. 2b, where three radial cracks have nucleated. At loads above the threshold, radial cracking in both materials were observed consistently, with corresponding acoustic emission. Similar behaviour was observed in the other materials tested.

Interpretation of the initially observed cracks as radial, rather than the manifestation of subsurface, penny-shaped median cracks breaking through to the surface is important, and is based on the following considerations. First, the cracks in NaCl are clearly radial. Additionally, study of cleaved indentations in single crystal α-SiC (reported elsewhere [8]) shows that radial cracks in this material definitely form in lieu of subsurface median cracks, for loads as high as 3500 g. Presently unreported results (this laboratory) of serial sectioning through cracked indents in polycrystalline Al_2O_3 show that in this material as well, initial indentation fractures are shallow radial surface cracks. Finally, acoustic emission was never obtained in any of the five materials studied for loads below which apparent radial cracks were first visible in the SEM. Since in the several cases cited above (NaCl, SiC, Al_2O_3) these cracks were proven to be radial, it is reasonable to suppose that those which in Si and Ge likewise appeared only in coincidence with the threshold acoustic emission, also were radial.

The acoustic emission associated with radial cracking occurred predominantly upon immediate application of the load; very little stress wave activity took place during the period in which the indenter rested upon the specimen. Moreover, except for fairly high loads, little acoustic response was seen as the load was removed. In these latter cases, the emission had two possible sources: (1) extension of the radial cracks formed on loading; (2) nucleation of lateral cracks. This point will be the subject of work to be reported later. However, since the counts on unloading constituted such a very small fraction of the total emission (loading plus unloading), the acoustic emission counts to be reported represent those detected within approximately the first half second of load application.

These results are summarized in Fig. 3, where P is the quasi-static load, and N the average number of total counts accumulated during a series of indentations at each load. It can be seen that for each ceramic, N decreases with P until a threshold value in load is reached. This point, indicated by the arrows along the horizontal axis, was defined in two ways: for Si and Ge, it corresponds to the load at which cracking, hence acoustic emission, is so infrequent that the average number of

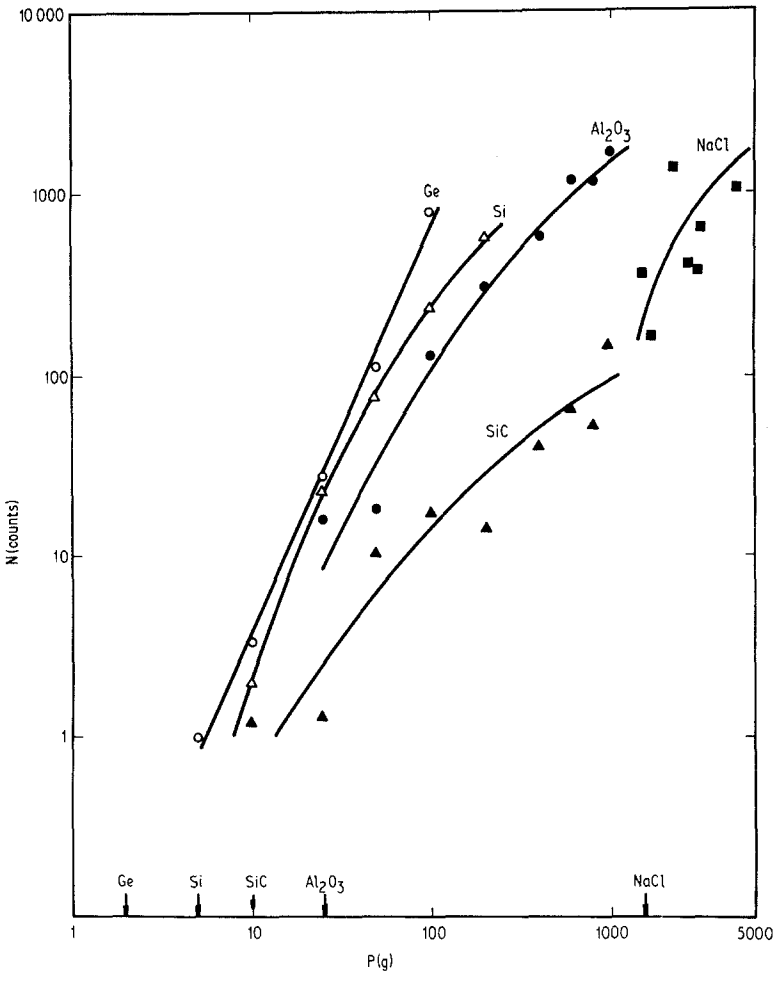

Figure 3 Acoustic emission counts versus indentation load for various ceramics.

emission counts is less than one. On the other hand, it was determined for Al_2O_3, SiC, and NaCl to be simply the load below which no acoustic emission (and no cracks as well) could be detected. It should be emphasized that scanning electron microscopy was used to verify the presence of at least one radial crack at each indentation for which acoustic emission was detected, and conversely, the absence of cracks at all "quiet" indents.

In addition to establishing the threshold load for cracking, which ranges from approximately 2 to 1500 g, the data of Fig. 3 also rank the ceramics in terms of their resistance to indentation crack nucleation. The least crack resistant material, insofar as concerns the load to produce a crack, is Ge, followed in order of increasing resistance by Si, SiC, Al_2O_3 and NaCl.

The SEM measurements of crack length and indentation dimension also were plotted, as shown for SiC in Fig. 4. There the crack length ($2c$) is considered to consist of the radial corner cracks plus the length of the indentation ($2a$). As seen in the figure, this procedure gives remarkably good load/crack length correlation, despite the fact that the corner cracks apparently do not actually penetrate the indent at low loads. For all materials studied, it was found that the indenter load P could be related to a and c over the entire load range by [5]

$$P/a^2 = 2H \tag{1}$$

and [6]

$$P/c^{3/2} = \beta_0 K_c, \tag{2}$$

where H is the hardness, K_c is the fracture toughness, and β_0 an indenter constant.

Threshold crack nucleation parameters are summarized for each material in Table I. Here

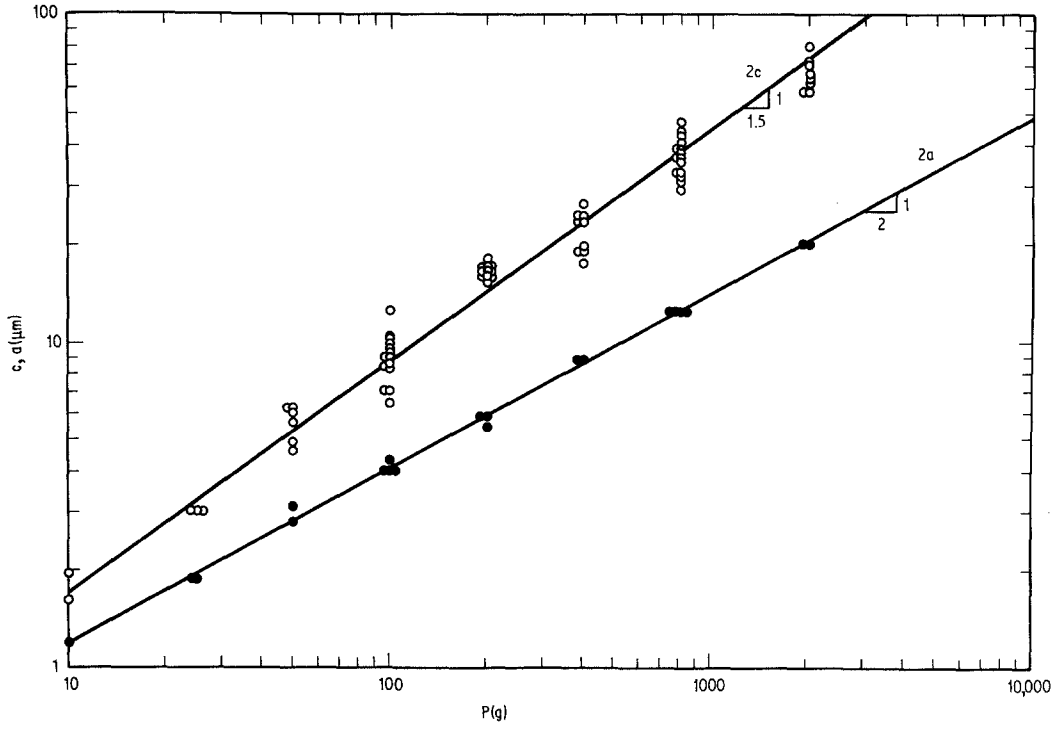

Figure 4 Crack length and indentation dimension versus indentation load for polycrystalline SiC.

P^*_{exp} is the lowest indenter load for which cracking occurred, as determined by SEM and AE, and c^*_{exp} is the length of the individual radial cracks corresponding to the values of P^*_{exp}, i.e., excluding the uncracked indentation dimension. Included for comparison are the corresponding theoretical parameters P^*_{theory} and c^*_{theory} from the Lawn–Evans theory, with c^*_{theory} defined as the radius of a subsurface median crack. The relationship between the latter and a surface radial crack attached to an indentation corner is not obvious, so the crack dimension comparison in this case can only be an approximate one.

It should be noted that to the knowledge of the authors, almost no comparable experiments have been carried out regarding the crack nucleation threshold. The only apparent comparison is afforded by the very limited work of Sata *et al.* [7], who determined the indentation threshold in Si using replica TEM. They found P^* to be approximately 3 g, in fairly good agreement with the present value of 5 g.

4. Discussion

From the results reported above, it seems clear that in all of the materials studied, the first cracks to form, hence those associated with the threshold, are radial surface cracks. Moreover, the ordering of the materials by the Lawn–Evans theory is perfect with respect both to threshold load level and crack size, despite the fact that the theory is intended to apply to median crack nucleation. It is for this latter reason, however, that numerical inaccuracies in P^*_{theory} arise.

According to Lawn and Evans [1] the threshold parameters are given by

$$c^*_{theory} = (1.767/\theta^2)(K_c/H)^2, \quad (3)$$

and

$$P^*_{theory} = (54.47\alpha/\eta^2\theta^4)(K_c/H)^3 K_c \quad (4)$$

where θ, η, and α are dimensionless factors related, respectively, to the peak stress at the elastic–plastic boundary beneath the indenter, the spacial extent of the tensile field, and the indenter geometry. Agreement between the predicted and observed crack sizes is quite good (Table I). In the case of P^*, however, the predicted values disagree with experimental observations by a considerable margin.

This disagreement can be rationalized by appealing to the theoretical model of Perrott [2]. We have already shown that the cracks nucleated in this study were radial, as required by the model. However, rigorous application of this analysis

requires that two other conditions be met as well, namely (1) that considerable subsurface plasticity must be present, and (2) in order for the hoop stress in the near-surface region to achieve tensile character, the surface plastic zone must be sufficiently large, i.e. approximately 50% larger than the indentation impression. We have addressed the first of these qualifications for the particular case of SiC, using a new technique (selected-area electron channelling) as described in detail elsewhere [8], with the principal conclusion that the extent of the subsurface plastic zone beneath an indentation in silicon carbide is quite large, equal to approximately five times the impression radius. The second requirement has been established through the recent TEM observations of Hockey *et al.* [9], in which the near-surface plastic zone radius was found, for SiC, Al_2O_3, and MgO (hence NaCl), to be clearly in excess of the minimum dimension required by the Perrott theory. For Si and Ge, it was found that near-surface plasticity was present at distances from the indent which were in the neighbourhood of the minimum.

Assuming, then, that the Perrott model is indeed applicable in the present case, the threshold loads calculated by Lawn and Evans must be modified. Specifically, Perrott showed that the maximum tensile stress across the subsurface median plane beneath the indent apex is actually lower than that acting across surface radial planes by a factor of $(1-2\nu)/(7-2\nu)$, or approximately 13. In addition, it is clear that based on the TEM observations of Hockey *et al.* [9], the value of $\eta(=1)$ used by Lawn and Evans is too large for Si and Ge. This parameter is related to the extent of the surface tensile field embedded within the near-surface plastic zone created by compressive stresses; considering the minimal size of their observed [8] surface zones, a value of $\eta \simeq 0.1$ would appear more appropriate for silicon and germanium. Applying these corrections to the Lawn–Evans data produces the results shown in Table I as $P^*_{\text{theory(corrected)}}$. In this case, quite satisfying agreement is now obtained between theory and experiment.

These results indicate that the Lawn–Evans approach to the indentation threshold cracking problem is essentially correct, but errs in its assumption of subsurface median cracking as the threshold event (at least for the materials studied). Basically, instead of a situation in which the subsurface plastic zone "searches" for pre-existing subsurface nucleation centres, one envisages a near-surface plastic zone "searching" for surface flaws. This arises from the unexpectedly large degree of plasticity apparently associated with indentations in even such strong, hard ceramics as SiC, and which alters the indentation stress distribution to the extent that the Perrott model must be invoked. However, the critical dependence of the cracking threshold upon H and K_c is not thereby affected, so that the (qualitative) ordering of materials in terms of their threshold loads for cracking is valid regardless.

Considering the good agreement between c^*_{exp} and c^*_{theory}, it seems clear that the *cracks* created at the threshold should be considered to be the small radial ones attached to the indentations. However, from the fracture mechanics–lifetime prediction point of view, the *flaw* created at the threshold may be significantly larger. The flaw probably should be considered to be a continuous shallow surface crack consisting of the radial crack segments plus the central, uncracked indentation. This is borne out by the experimentally obtained relationship between load and total crack length $2c$ summarized in Fig. 4. Since the threshold for cracking is determined by the lowest loads and smallest cracks plotted in Fig. 4, the remainder of the load–crack length results should be concerned with propagation. Indeed, Equation 2, which describes these data, has precisely the same form as the fracture mechanics equation for equilibrium penny-like cracks extending under centre-loading conditions [6]. The fact that there is no break in plots like Fig. 4 as loads are increased above the threshold value thus implies that the very smallest indentation-induced flaws, although well within the indentation field of influence, behave like large flaws whose cracked region is much larger than the nucleating indentation. From the fracture mechanics point of view, they therefore are analytically treatable in the same fashion.

5. Conclusions

The ordering of various ceramics with regard to their relative threshold loads and crack sizes during indentation microfracture is shown to be accomplished successfully by the theory of Lawn and Evans, although at the threshold, radial surface, rather than the predicted median subsurface, cracks, are observed. Moreover, the sizes of the threshold cracks are predicted with reasonable accuracy. The cracking threshold load, however, is

in error by more than an order of magnitude, a factor which can be corrected by taking into account indentation plasticity and the indentation stress field analysis of Perrott. It appears that fracture mechanics relationships may be applicable without alteration from the macroscopic surface crack regime down to the very threshold for indentation crack nucleation.

Acknowledgement

The authors are grateful for the support of the Office of Naval Research, Contract no. N00014-75-C-0668, during the course of this work.

References

1. B. R. LAWN and A. G. EVANS, *J. Mater. Sci.* **12** (1977) 2195.
2. C. M. PERROTT, *Wear* **45** (1977) 293.
3. J. LANKFORD, "Fracture Mechanics of Ceramics, Vol. 3, edited by R. C. Bradt, D. P. H. Hasselman and F. F. Lange (Plenum, New York, 1978) p. 245.
4. B. J. HOCKEY, "The Science of Hardness Testing and its Research Applications", edited by J. H. Westbrook and H. Conrad (American Society for Metals, Metals Park, Ohio, 1973) p. 30.
5. B. R. LAWN, T. JENSEN and A. ARORA, *J. Mater. Sci.* **11** (1976) 575.
6. B. R. LAWN and E. R. FULLER, *ibid* **10** (1975) 2016.
7. T. SATA, K. TAKAMOTO and H. YOSHIKAWA, *Bull. Jap. Soc. Prec. Eng.* **3** (1969) 13.
8. J. LANKFORD and D. L. DAVIDSON, *J. Mater. Sci.* **14** (1979) 1669.
9. B. J. HOCKEY, S. M. WEIDERHORN and H. JOHNSON, "Fracture Mechanics of Ceramics", Vol. 3, edited by R. C. Bradt, D. P. Hasselman and F. F. Lange (Plenum, New York, 1978) p. 379.

Received 6 October and accepted 13 October 1978.